



OPEN Testosterone/androgen receptor antagonizes immobility-induced muscle atrophy through Inhibition of myostatin transcription and inflammation in mice

Miya Oura¹, Bo-Kyung Son^{1,2,3}✉, Zehan Song¹, Koichi Toyoshima¹, Michiko Nanao-Hamai¹, Sumito Ogawa¹ & Masahiro Akishita¹

Sarcopenia is caused by excessive muscle protein degradation owing to various factors, including disuse. Although testosterone supplementation is an effective treatment, the underlying molecular mechanisms, particularly the role of the androgen receptor (AR), remain unclear. In this study, we examined the preventive actions of testosterone/AR against muscle atrophy in a murine model of immobilization-induced muscle atrophy. The bilateral hindlimbs of 8-week-old male C57BL/6J mice were immobilized using a wire. Testosterone deficiency and supplementation (50 µg/mL) were conducted by castration and intraperitoneal injection (twice a week for a month), respectively. The results showed a remarkable decline in muscle mass and strength after wire-induced immobilization for 14 days. The expression of muscle atrophic factors (Atrogin1 and MuRF1) and inflammatory factors (F4/80 and interleukin-6 (IL-6)) significantly increased ($p < 0.001$). Notably, muscular AR expression significantly decreased, whereas myostatin and CCAAT/enhancer-binding protein delta (C/EBP δ), a transcriptional activator of myostatin, were significantly elevated ($p < 0.05$). After castration, AR expression further decreased, and muscular changes with wire-induced immobilization deteriorated. These exacerbations were completely ameliorated by testosterone supplementation and AR upregulation. Our study provides important therapeutic insights into testosterone/AR in muscular atrophy caused by immobilization and shows that muscular AR in a testosterone-dependent manner regulates C/EBP δ /myostatin and inflammation.

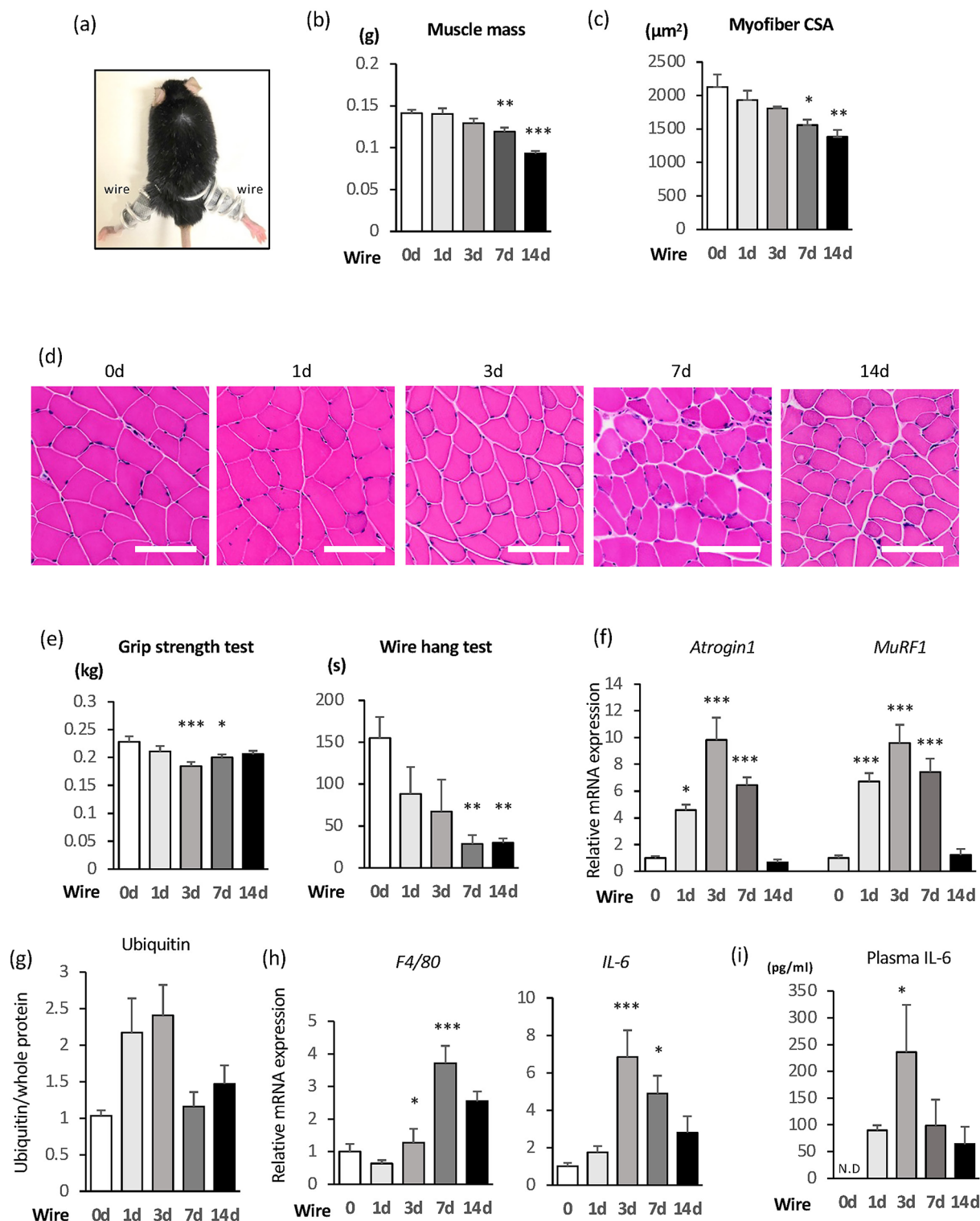
Keywords Androgen receptor, Inflammation, Male, Myostatin, Sarcopenia, Testosterone

Skeletal muscle mass, muscle strength, bone density, and motor coordination capacity decrease with age, leading to a decline in physical function¹. These changes result in a decrease in the patients' quality of life and increase the risk of falls, nursing home admissions, and complications, ultimately leading to a worse life expectancy.

Age-related loss of skeletal muscle mass and strength, specifically referred to as sarcopenia, is defined as a progressive systemic skeletal muscle disorder with accelerated loss of muscle mass and function². Immobilization-induced muscle atrophy, one of the major causes of secondary sarcopenia, is caused by the mechanical unloading of skeletal muscles due to excessive rest and inactivity. Inhibition of muscle synthesis by insulin-like growth factor 1 (IGF-1) resistance, increased inflammatory cytokines, and activation of the myostatin signaling pathway trigger the expression of the atrogenes MuRF1 and Atrogin1, which are responsible for muscle atrophy via the ubiquitin-proteasome system³. In fact, elderly patients with sarcopenia have significantly higher levels of blood high-sensitive C-reactive protein (hsCRP)⁴ and inflammatory cytokines such as interleukin-6 (IL-6) and tumor necrosis factor- α (TNF α) compared to healthy elderly patients⁵. These inflammatory cytokines contribute to the development of sarcopenia by modulating key regulatory factors, such as MyoD and myostatin, thereby disrupting the balance between muscle protein synthesis and degradation^{6,7}. Chronic inflammation induced by

¹Department of Geriatric Medicine, The University of Tokyo, 7-3-1 Hongo, Bunkyo-ku, Tokyo 113-8655, Japan.

²Institute for Future Initiatives, Institute of Gerontology, The University of Tokyo, Engineering 8th Building 709, 7-3-1 Hongo, Bunkyo-ku, Tokyo 113-8655, Japan. ³Institute of Gerontology, The University of Tokyo, 7-3-1 Hongo, Bunkyo-ku, Tokyo 113-8655, Japan. ✉email: son@iog.u-tokyo.ac.jp; sontky72@g.ecc.u-tokyo.ac.jp



aging is termed “Inflammaging,” which has recently received attention as an underlying pathology for various geriatric diseases such as sarcopenia^{8–10}.

Testosterone is a major male sex hormone that has various effects on target organs, such as the prostate, muscles, bones, adipose cell tissue, and brain. Low testosterone levels can cause obesity and reduce physical function, muscle strength, and mass^{11,12}. Conversely, testosterone administration promotes muscle anabolism, even in elderly individuals, and inhibits muscle atrophy in elderly individuals with low testosterone levels¹³. Testosterone has been shown to affect both the synthetic and degradative systems in muscles¹⁴ and regulation of the ubiquitin-proteasome system for muscle proteolysis¹⁵. Various pathways are already known such as IGF-1, PI3K/Akt, and Akt/mTORC1/Foxo3a signaling^{16–19}. Furthermore, testosterone suppresses the expression of inflammatory cytokines, including IL-6, via the androgen receptor (AR)^{20,21}.

◀ **Fig. 1.** Mouse hindlimb immobilization induces muscle degradation and inflammatory response. (a) Mouse hindlimb immobilization model. (b) The gastrocnemius weight significantly decreased within 1 week after immobilization ($n = 6/\text{group}$). (c) The gastrocnemius cross-sectional area (CSA) significantly decreased within 1 week after immobilization ($n = 4/\text{group}$). (d) HE stained images of gastrocnemius transverse section (scale bars: 100 μm). (e) Grip strength test and wire hang test were performed to measure the muscle strength of the four limbs of mice, and both showed a significant decrease within 1 week after immobilization ($n = 6/\text{group}$). (f) The expression of degradation-related genes in the gastrocnemius muscle was maximal within 3 days after immobilization and then peaked out ($n = 6/\text{group}$). (g) Quantification of WB results confirm that ubiquitin expression in the gastrocnemius muscle ($n = 3/\text{group}$). The original blots are presented in Supplementary Fig. S3. (h) The expression of inflammation-related genes in the gastrocnemius muscle was maximal within 1 week after immobilization and then peaked out ($n = 6/\text{group}$). (i) The IL-6 levels in blood were maximal within 3 days after immobilization and then peaked out ($n = 4/\text{group}$). All values are presented as the mean \pm SEM. * $p < 0.05$, ** $p < 0.01$, *** $p < 0.001$, vs. Wire 0d, one-way ANOVA with post hoc Tukey test.

The AR is a ligand-dependent nuclear transcription factor that binds to androgen response elements (AREs) and regulates the transcription of target genes through several co-regulators. Since the AR is expressed in a variety of cell types in mammalian skeletal muscles (e.g., motoneurons, fibroblasts, satellite cells, and myofibers)^{22–24}, all of these cells are potential sites for testosterone²⁵.

AR deficiency in the skeletal muscles reduces muscle strength^{25,26}. We recently found that exercise-mimicking electric pulse stimulation (EPS) of C2C12 myotubes increases testosterone levels and AR expression²⁷. Therefore, testosterone and AR regulate important pathways in atrophy progression, and inflammation and degradation markers could be potential candidates for responsive target molecules; however, the detailed mechanism remains unclear.

In this study, we aimed to determine the roles of testosterone and the AR in the progression of muscle atrophy, including their downstream mechanisms, using a murine model of immobilization-induced muscle atrophy.

Results

Mouse hindlimb immobilization induces muscle degradation and inflammation

A hindlimb immobilization model was established using 10-week-old male C57BL/6J mice, as described above (Fig. 1a). Muscle weight, muscle cross-sectional area (CSA), and muscle strength were measured at immobilized periods of 0, 1, 3, 7, and 14 days. The gastrocnemius weight and CSA tended to decrease over time from the start of immobilization, and both showed a significant decrease within 1 week (Fig. 1b–d). The weight of the soleus muscle showed a similar trend (Supplementary Fig. S1). The muscle strength also significantly decreased within 1 week (Fig. 1e). These findings confirm that hindlimb immobilization with wires represents a suitable atrophy model to exhibit a decrease in muscle mass and whole-limb strength in mice.

Next, using the gastrocnemius muscle tissue from this murine model, we measured changes in the expression of degradation- and inflammation-related genes at the mRNA level.

Both Atrogin1 and MuRF1, which are related to degradation, were upregulated early after the start of immobilization, reaching maximum expression on day 3, and then peaking (Fig. 1f). A similar trend was observed for ubiquitin expression (Fig. 1g). These results support the phenotypic changes of decreased muscle weight and CSA associated with hindlimb immobilization.

Similarly, among the inflammation-related genes, F4/80 (a major marker of mature macrophages in mice) and IL-6 (a pro-inflammatory cytokine) increased within 1 week after the start of fixation and then peaked (Fig. 1h). The blood levels of IL-6 also increased (Fig. 1i).

Thus, changes in the gene expression of degradation and inflammatory factors occurred very early after disuse. In addition, the degradation and inflammatory factors were found to change simultaneously, suggesting the involvement of inflammation in the degradation process during disuse.

Decrease in AR protein expression in hindlimb immobilization

Since a decrease in testosterone causes muscle atrophy^{11,12} and testosterone acts through the AR, we hypothesized that the expression or activity of AR may decrease during the process of muscle atrophy.

Therefore, we next analyzed the changes in AR expression in the immobilization-induced muscle atrophy model by WB. The results showed that AR expression significantly decreased 3 days after immobilization with the progression of immobilization-induced muscle atrophy (Fig. 2a, b), although no manipulation was performed to cause direct increase or decrease in testosterone (exogenous testosterone supplementation or castration).

Our previous study showed that CCAAT/enhancer-binding protein delta (C/EBP δ), which is a member of the C/EBP family of transcriptional regulators²⁸ and known as a transcription factor involved in muscle degradation by the ubiquitin-proteasome system, was suppressed with increased AR expression²⁷. C/EBP δ is also a transcriptional regulator of IL-6 and myostatin, suggesting that a positive feedback loop between IL-6 and C/EBP δ could be a possible mechanism. The expression of FOXO1 and FOXO3a, transcription factors that induce muscle atrophy by proteolysis and cooperate with C/EBP δ , increased in parallel, indicating an effect associated with the elevated expression of C/EBP δ (Supplementary Fig. S2). Moreover, in the immobilization-induced muscle atrophy model, gene expression of myostatin, which is downstream of C/EBP δ and signaling pathways, was increased at approximately the same time as the decreased expression of AR (Fig. 2c).

These results suggest that during the process of immobilization-induced muscle atrophy, AR expression decreased and the C/EBP δ -myostatin-IL-6 pathway was upregulated to counterbalance it, leading to progressive muscle degradation.

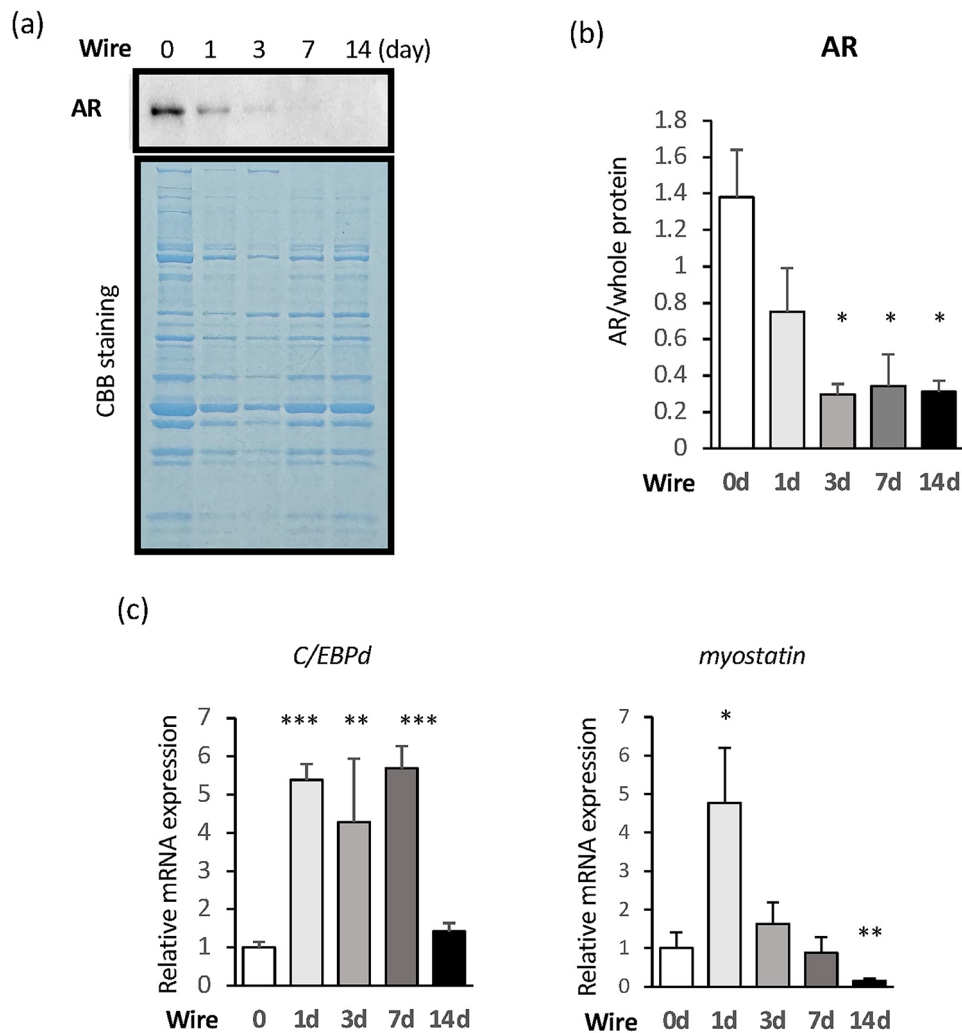


Fig. 2. Mouse hindlimb immobilization induces a significant decrease in AR protein expression. **(a)** WB results confirm that AR expression in the gastrocnemius muscle is reduced with disuse muscle atrophy. The original blots are presented in Supplementary Fig. S4. Coomassie brilliant blue (CBB) staining is seen using the same protein samples. **(b)** Quantification of WB results ($n = 5-6$ /group). **(c)** Increased expression of C/EBPδ, a transcriptional regulator of AR, and myostatin, located downstream of the signaling pathway, was observed ($n = 6$ /group). All values are presented as the mean \pm SEM. * $p < 0.05$, ** $p < 0.01$, *** $p < 0.001$, vs. wire 0d, one-way ANOVA with post hoc Tukey test.

Castration accelerates immobilization-induced muscle atrophy and AR downregulation

To examine the effects of the AR, we conducted an experiment combining castration- and immobilization-induced muscle atrophy to exclude the effects of endogenous testosterone. This combined model (castration + immobilization) was created by removing the testes of 8-week-old male C57BL/6J mice, followed by hindlimb immobilization 4 weeks later. The gastrocnemius weight and muscle strength of mice were measured at fixation periods of 0, 1, 3, 7, and 14 days (Fig. 3a). The gastrocnemius weight tended to decrease with time after the start of immobilization in each group. Compared to the sham group at each fixation period, the castration alone group showed a significant decrease in gastrocnemius weight only in the 3- and 7-day post-immobilization group, but not in the other groups. In contrast, the castration + immobilization group showed the most pronounced decrease from 1 day after immobilization, and the decrease remained consistent until 14 days after fixation (Fig. 3b). A further decrease was observed for muscle strength. In the grip strength test, the castration alone group showed a significant decrease in the before fixation, but only the fixed 7-day group showed a significant decrease, whereas the castration + immobilization group showed the most pronounced decrease from 1 day after immobilization, and the consistent decline was seen by 14 days after fixation. In the wire hang test, only the castration + immobilization group showed a consistent decline after 3 days of immobilization (Fig. 3c). To summarize, the combined model (castration + immobilization) shows an additive decline, and the degree increases as the time of immobilization periods.

For subsequent molecular analysis, based on previous results in which a significant decrease in AR associated with immobilization was observed within 3 days and a steady decrease thereafter, the time points were focused

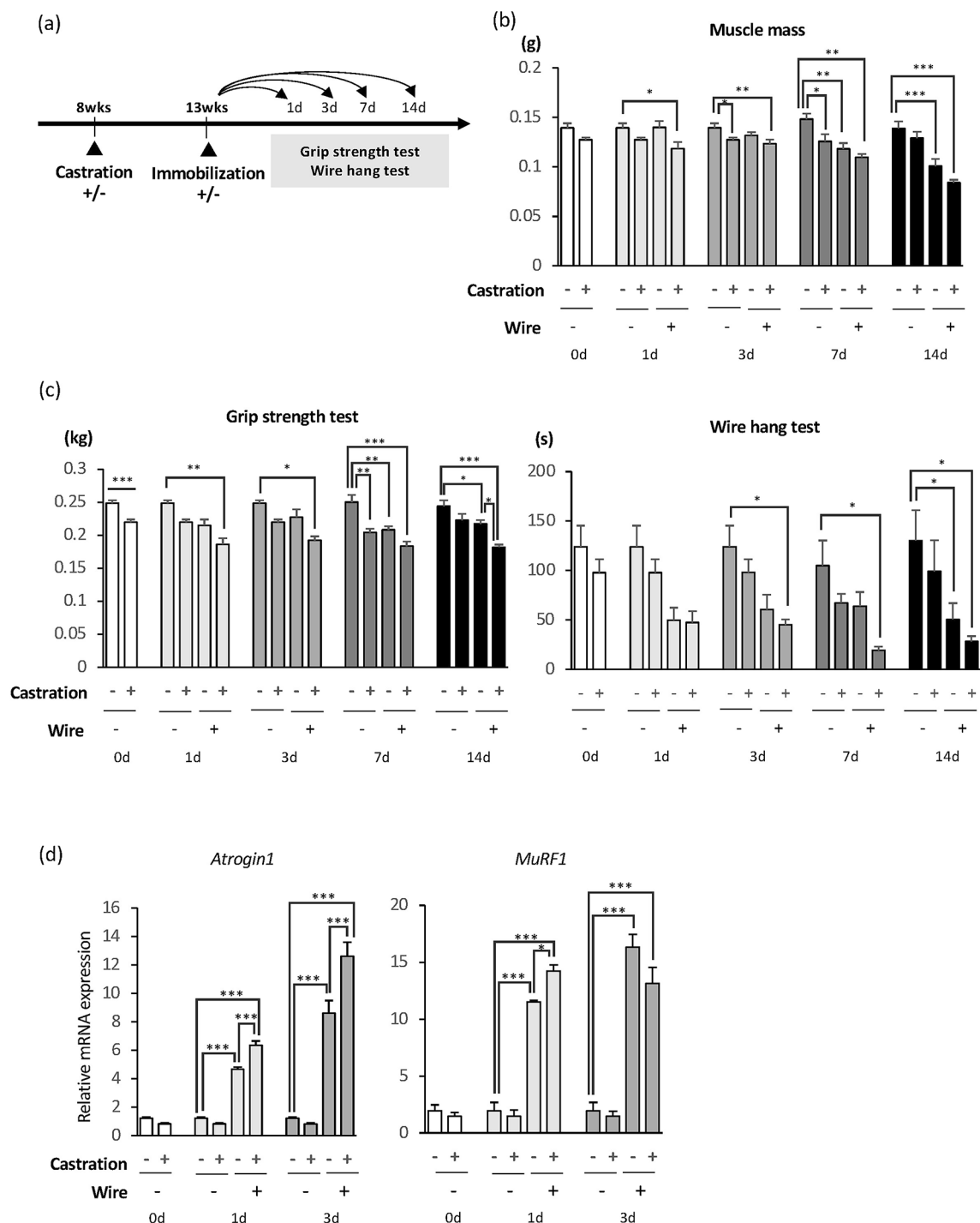


Fig. 3. Castration accelerates disuse muscle atrophy. **(a)** Experimental design of castration and immobilization. **(b,c)** Both the gastrocnemius weight and muscle strength showed the earliest and largest decline in the castrated mice with hindlimb immobilization-group ($n=4-8/\text{group}$). **(d)** Expression of degradation-related genes in the gastrocnemius muscle increased in conjunction with disuse ($n=4-7/\text{group}$). All values are presented as the mean \pm SEM. * $p < 0.05$, ** $p < 0.01$, *** $p < 0.001$, Mann-Whitney U test or one-way ANOVA with post hoc Tukey test.

on 0, 1, and 3 days. Atrogin1 expression was upregulated in the immobilization and castration + immobilization groups at 1- and 3- days post-immobilization compared to the respective sham groups, and the extent of the upregulation was highest in the castration + immobilization group. As for MuRF1, an increase was observed in the immobilization and castration + immobilization groups on days 1 and 3, respectively, and at day 1, the largest increase was observed in the castration + immobilization group (Fig. 3d). These results support an immobilization-induced muscle atrophy phenotype.

AR expression was significantly decreased at 1 and 3 days of castration + immobilization group, compared to immobilization alone group (Fig. 4a, b). At the same time, the expression of myostatin and C/EBP δ , a transcriptional regulator of AR was significantly increased. C/EBP δ expression was upregulated in the immobilization and castration + immobilization groups at 1- and 3- days post-immobilization compared to the respective sham groups, and at day 1, the largest increase was observed in the castration + immobilization group. As for myostatin, an increase was observed in the immobilization and castration + immobilization groups on day 3 (Fig. 4c). These results suggest a detrimental effect of castration on the pathological condition as muscle atrophy caused by immobilization and support the hypothesis that the pathway between AR and C/EBP δ is involved in immobilization-induced muscle atrophy.

In the inflammatory system, the expression levels of IL-6 and macrophages were elevated in the castration + immobilization group. IL-6 expression was upregulated in the immobilization and castration + immobilization groups at 1- and 3- days post-immobilization compared to the respective sham groups (Fig. 4d). For F4/80, a significant increase was observed in the castration + immobilization group on day 3 (Fig. 4e). Similarly, IHC showed a significant increase in CD68 expression in the castration + immobilization group on day 3 (Fig. 4f, g). These results suggest the involvement of inflammation in the muscle degradation process in immobilization-induced muscle atrophy, which may be aggravated by a detrimental effect of castration, as mentioned above.

Testosterone supplementation improves muscle atrophy and inflammation deteriorated by immobilization and castration

To evaluate the effects of testosterone on immobilization-induced muscle atrophy, testosterone was administered to castrated mice with immobilization-induced muscle atrophy (Fig. 5a). The control group in this experiment was the vehicle group under castration + immobilization conditions. The results showed that on days 0, 1, and 3 after hindlimb immobilization, the muscle weight and strength were restored by testosterone administration (Fig. 5b, c). Among the degradation-related genes, Atrogin1 showed increased expression on days 1 and 3 after immobilization compared to the sham group on day 0, but this change was counteracted by testosterone replacement on day 3. In contrast, MuRF1 was not significantly decreased by testosterone supplementation (Fig. 5d). Furthermore, testosterone supplementation significantly increased the expression of AR from days 0 to 3, which was significantly higher than that in the castration + immobilization + vehicle group (Fig. 5e, f). C/EBP δ was also significantly lower in the castration + immobilization + vehicle group than in the castration + immobilization + testosterone group on day 0 due to testosterone pre-supplementation. A significant decrease in C/EBP δ expression was also observed up to days 1 and 3. In contrast, no significant decrease was observed in myostatin expression on day 0, but on days 1 and 3, a significant decrease in expression was shown by testosterone supplementation compared to the castration + immobilization + vehicle group (Fig. 5g, h). These results suggest that the AR-mediated enhancement of the C/EBP δ pathway is still involved in the process of immobilization-induced muscle atrophy.

Discussion

In this study, using a mouse model of immobilization-induced muscle atrophy, we showed that reduced AR correlated to muscle atrophy as a result of an increase in C/EBP δ expression (a transcription factor of myostatin), followed by an increase in IL-6. These AR-mediated regulatory pathways were further impaired by castration and reversed by testosterone supplementation.

In the skeletal muscles, AR has been investigated in various ways using myocyte-specific AR knockout (mARKO) mice. One study demonstrated that myocytic AR controls muscle strength, but not muscle mass²⁵. Another study demonstrated that myocytic AR contributes to the maintenance of muscle mass, but not muscle strength²⁶. Thus, the role of the muscular AR remains controversial. In the present study, we examined the regulatory effects of testosterone and AR on muscle atrophy. We found that both muscle strength and mass were regulated in parallel with the AR under conditions of testosterone deficiency or supplementation. Thus, our murine model can clarify the effects of testosterone/AR on muscle atrophy. However, the grip strength and wirehang tests used to assess muscle strength in this study measured whole-limb strength, rather than specifically targeting hindlimb strength. Future studies are needed to develop more accurate methods for assessing the effects of hindlimb immobilization.

In this mechanistic study, we found that downregulation of the AR is associated with upregulation of C/EBP δ –myostatin. Recently, myostatin (a member of the TGF β superfamily) has been proposed as an important molecule responsible for regulating the muscle proteolytic pathway. Overexpression of myostatin in adult mice causes severe muscle and fat loss, as observed in human cachexia syndrome, whereas mice and cows that are genetically deficient in myostatin exhibit dramatic increase in skeletal muscle mass, suggesting that myostatin inhibits muscle growth²⁹. Several substances that block the myostatin pathway have been developed, some of which have progressed to clinical trials; however, none are available yet³⁰. It may be difficult for a single molecule to inhibit the entire myostatin pathway, and this study suggests that the AR may be an upstream factor of myostatin. It has been reported that testosterone reduces myostatin levels¹⁹ and myostatin gene expression is directly upregulated via the AR at the transcriptional level³¹. Consistent with our findings, previous studies have shown that exogenous testosterone decreases muscle myostatin expression in a dose-dependent manner³² and that castration increases its expression³³. In addition to myostatin, recent studies on cellular metabolism in AR-deficient skeletal muscles have suggested alterations in ARE genes related to cellular metabolism such as glucose metabolism, fatty acid metabolism, and polyamine synthesis³⁴. These findings should be considered in future studies.

A further interesting finding in this study was that the expression of C/EBP δ increased as the AR expression decreased. Regarding the molecular regulation of myostatin, C/EBP δ is an important transcription factor of

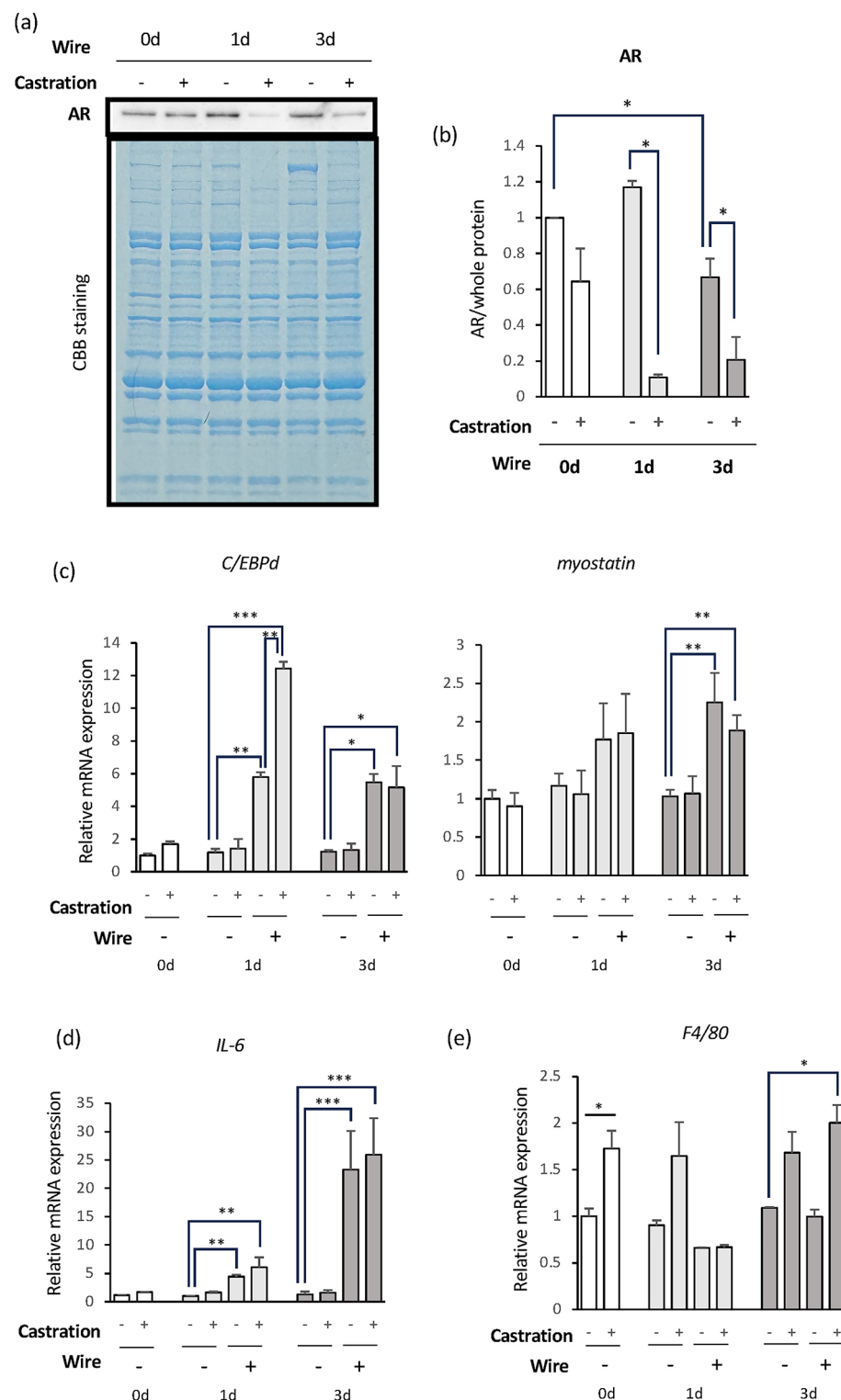


Fig. 4. Castration reduces AR protein expression. **(a)** WB results confirm that AR expression in the gastrocnemius muscle is reduced at both 1 and 3 days after immobilization. Original blots are presented in Supplementary Fig. S5. Coomassie brilliant blue (CBB) staining is seen using the same protein samples. **(b)** Quantification of WB results ($n=4-7/\text{group}$). **(c)** Increased expression of *C/EBPδ* and *myostatin* was observed in conjunction with decreased expression of AR ($n=4-7/\text{group}$). **(d)** Increased expression of *IL-6* was observed in conjunction with decreased expression of AR ($n=4-7/\text{group}$). **(e)** Increased expression of *F4/80* was observed in conjunction with decreased expression of AR ($n=4-7/\text{group}$). **(f)** Immunohistochemical analysis of CD68+ macrophage. **(g)** Quantification of CD68+ macrophage cells ($n=2-4/\text{group}$). All values are presented as the mean \pm SEM. * $p < 0.05$, ** $p < 0.01$, *** $p < 0.001$ vs. Sham Wire, Mann-Whitney *U* test or one-way ANOVA with post hoc Tukey test.

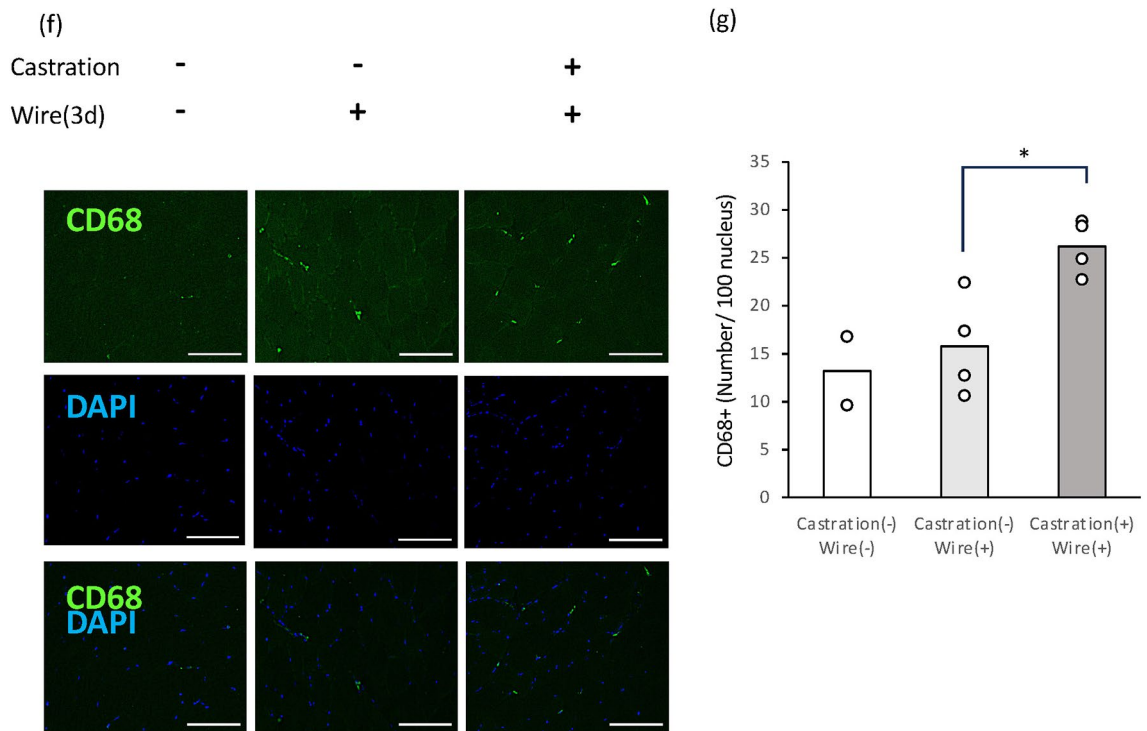


Figure 4. (continued)

myostatin, as well as the known Akt and mTOR signaling pathways¹⁶, which binds to C/EBP binding element (CBE) in the promoter region³⁵. C/EBP δ is upregulated in skeletal muscle in response to glucocorticoids³⁶ and its DNA-binding activity is also increased by glucocorticoids³⁷. C/EBP δ KO mice show resistance to cancer cachexia and muscle atrophy associated with chronic kidney disease²⁸.

Given that both ARE and CBE exists in the promoter region of myostatin, it is conceivable that AR and C/EBP δ may act cooperatively in the transcriptional regulation of myostatin. Supporting this notion, our recent report demonstrated that an increase in AR expression and decrease in C/EBP δ expression were observed in EPS-stimulated C2C12 cells. Furthermore, flutamide (an AR inhibitor) reversed the decreased in C/EBP δ expression²⁷, suggesting an AR-mediated regulation mechanism of C/EBP δ expression. At the same time, myostatin is known to be regulated not only by C/EBP δ but also by other signaling pathways. In a previous report using mouse C2C12 myoblasts, FOXO1, and SMAD transcription factors were reported to bind to the myostatin promoter, and their overexpression caused a significant increase in myostatin promoter activity³⁸. In addition, some feedback may be received from downstream myostatin-regulated pathways such as Akt and mTOR¹⁶. The multifactorial regulation of myostatin may account for the differing behavior of C/EBP δ , and its impact over time will be explored in future studies.

Inflammatory cytokines, including IL-6, cause skeletal muscle atrophy and sarcopenia³⁹. IL-6 and TNF α contribute to the progression of muscle atrophy by disrupting the balance between muscle protein synthesis and degradation systems^{6,7} and can promote inflammatory cell infiltration via the NF- κ B system, leading to deterioration of muscle quality⁴⁰. Interestingly, several previous reports have shown that the C/EBP δ and myostatin also cause an increase in IL-6 via pathways such as p38 MAPK and MEK1^{7,41}. In particular, since C/EBP δ enhances the production of inflammatory cytokine such as IL-6, modulates macrophage function, and increases inflammatory responses⁴². It also amplifies IL-6 signaling by directly targeting the IL-6 receptor gene⁴³, these factors may be involved in inflammation-mediated muscle atrophy. Testosterone exerts anti-inflammatory effects via the AR^{20,21}. Evidence from animal studies of castrated mice and clinical reports in older men have shown that low testosterone levels increase inflammatory cytokines and, conversely, testosterone supplementation decreases inflammatory cytokines⁴⁴. Our recent study investigating the effects of the AR on muscle inflammation showed that AR upregulation and IL-6 downregulation were observed in EPS-stimulated C2C12 cells, and that flutamide reversed IL-6 downregulation. As C/EBP-binding motifs exists in the promoter region of IL-6⁴⁵, a positive feedback loop between IL-6 and C/EBP δ may work, and thus the AR may induce inflammation via C/EBP δ ²⁷. Furthermore, given that IL-6 has diverse secretory patterns and actions^{46–48}, further investigation of AR-dependent IL-6 regulation is needed.

In this study, peak changes in all parameters, including AR expression, occurred early (3 days to 1 week) after disuse of the gastrocnemius muscle in the immobilization-induced muscle atrophy model. The early existence of a dynamic period of muscle strength and metabolic changes has been consistently observed in several previous studies^{46,49–51}, which might indicate the importance of early intervention. Thus, we expect that the effects and

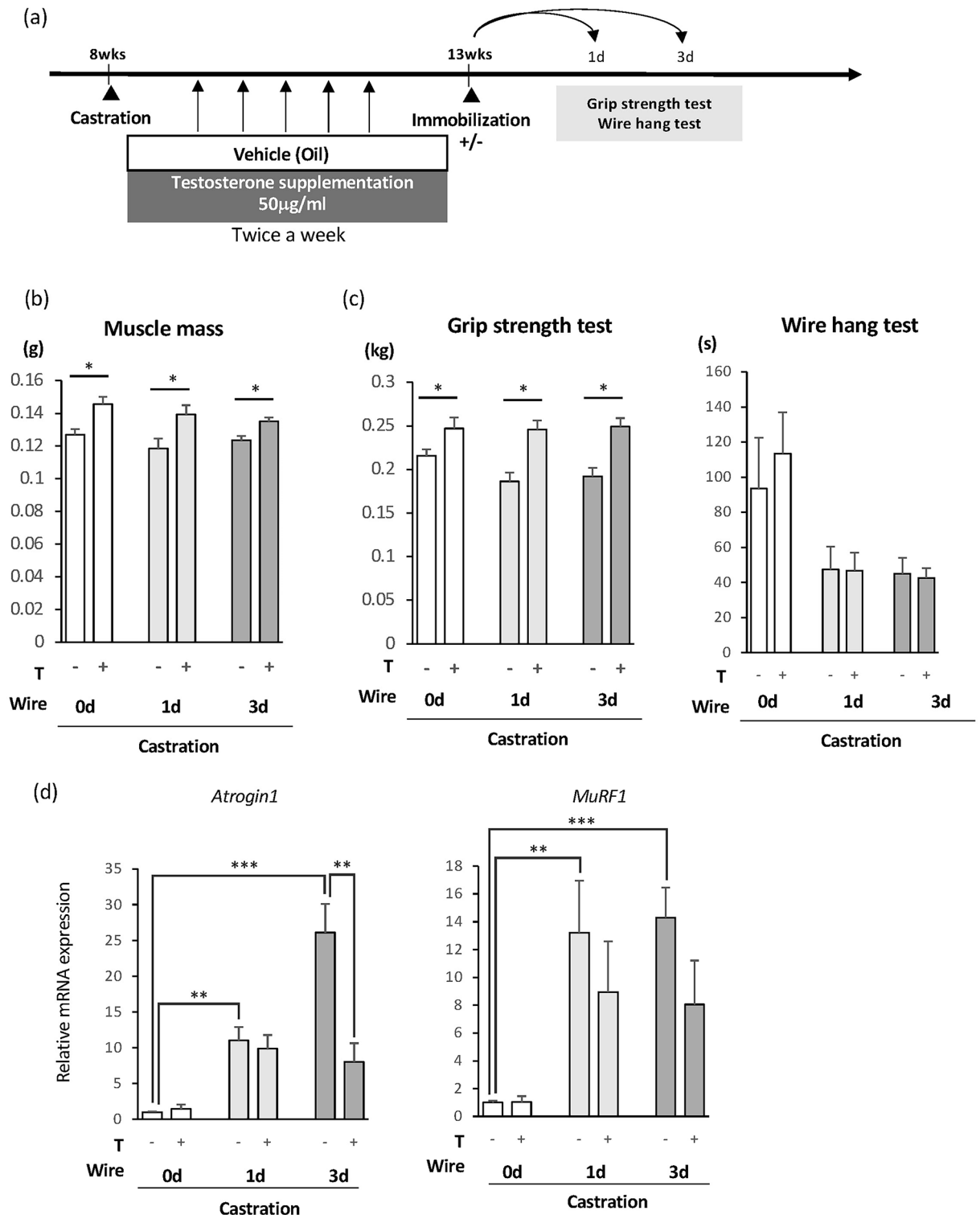


Fig. 5. Muscle atrophy and inflammation deteriorated by immobilization and castration improve following testosterone administration. **(a)** Experimental design of castration, testosterone administration, and immobilization. **(b,c)** Testosterone administration to mice with hindlimb immobilization after castration rescued the decrease in gastrocnemius weight and grip strength test ($n = 4-6/\text{group}$). **(d)** Testosterone administration suppressed the disuse-associated increase in degradation-related genes ($n = 4-10/\text{group}$). **(e)** Testosterone administration increased AR expression in the gastrocnemius muscle at any time point of 0, 1, and 3 days after immobilization. The original blots are presented in Supplementary Fig. S6. Coomassie brilliant blue (CBB) staining is seen using the same protein samples. **(f)** Quantification of WB results ($n = 4-6/\text{group}$). **(g,h)** Decreased expression of C/EBP δ , myostatin, F4/80, and IL-6 was observed in conjunction with increased expression of AR ($n = 4-10/\text{group}$). All values are presented as the mean \pm SEM. * $p < 0.05$, ** $p < 0.01$, *** $p < 0.001$ vs. testosterone (-), Mann-Whitney U test or one-way ANOVA with post hoc Tukey test.

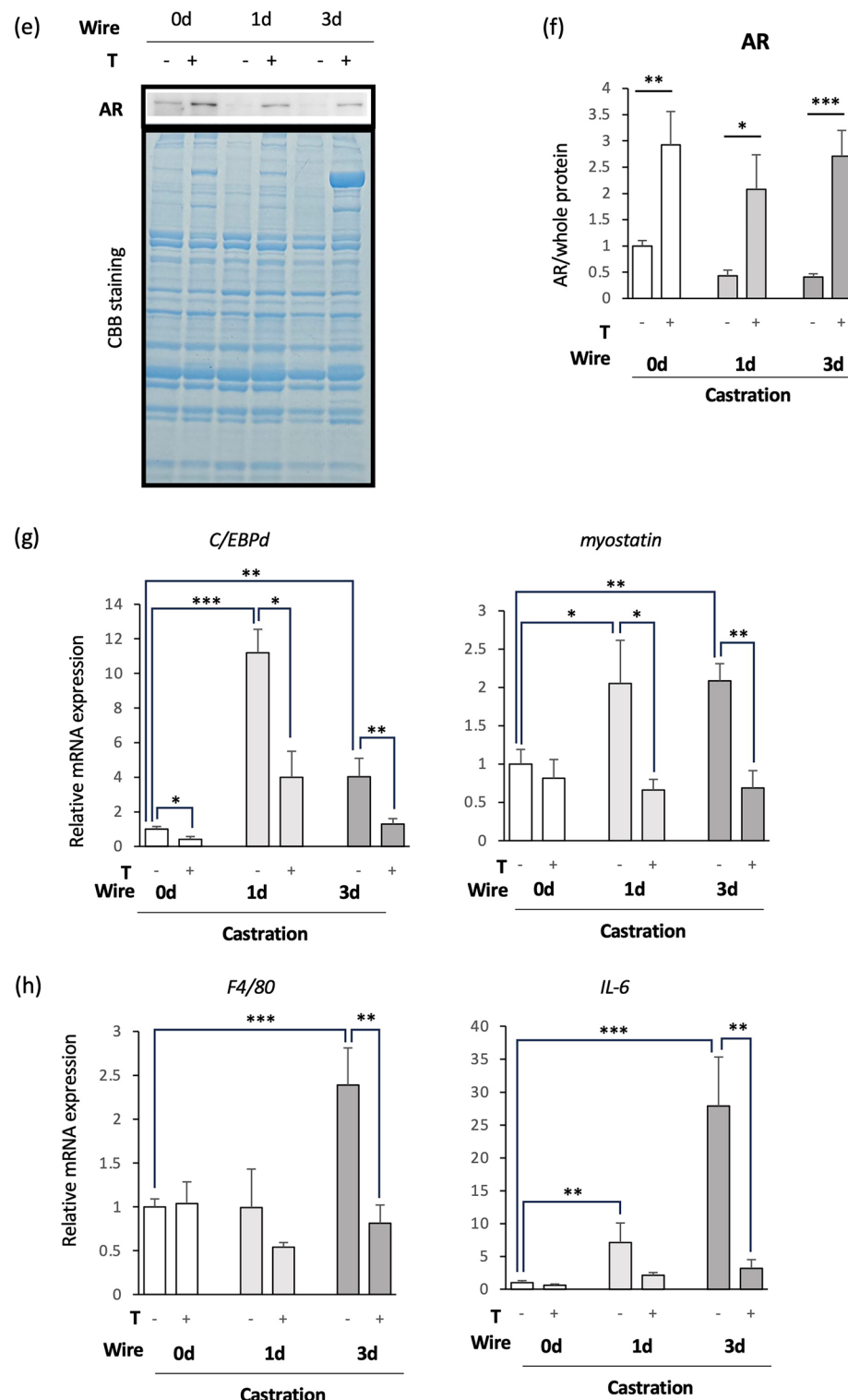


Figure 5. (continued)

limitations of early intervention and degree of reversibility will be examined in the future, which will be useful for the prevention and treatment of disuse-related muscle atrophy.

Based on our observations, testosterone supplementation and selective AR modulators (SARMs) are potential therapeutic agents for sarcopenia. Furthermore, with the same mechanistic insights into testosterone/AR regulation, low-intensity exercise preventing muscle atrophy has been suggested to be effective in sarcopenia²⁷. Thus, discussing why testosterone supplementation increased the AR and the relationship between testosterone secretion (in testicular-derived and/or in other tissue, including skeletal muscle-derived) and AR expression in

skeletal muscle, may provide future issues to consider in the treatment of sarcopenia with testosterone or SARM. Moreover, to prevent or treat sarcopenia, proactive clinical trials are needed to determine the effects of exercise (e.g., intensity, duration, and frequency) and develop pharmacological agents for testosterone or SARM.

In conclusion, using a mouse model of immobilization-induced muscle atrophy, we found that AR expression decreased with gastrocnemius muscle atrophy (fast twitch). It can be suggested that muscle atrophy is promoted through increased expression of the AR-related genes, C/EBP δ and myostatin, and inflammatory cytokines such as IL-6. This was evidenced by a further reduction in AR expression after castration, which was ameliorated by testosterone supplementation.

Methods

Animals

C57BL/6J male mice (Sankyo Labo Service Corporation, Inc., Tokyo, Japan) were housed with free access to water and standard rodent chow under a 12-h light/dark cycle at constant room temperature (21 ± 3 °C) and humidity ($40\% \pm 10\%$).

The mice were anesthetized with three different anesthetics (medetomidine hydrochloride, midazolam, and butorphanol) according to the protocol recommended by the Animal Experiment Committee of the University of Tokyo⁵². At the time of euthanasia after the experiment, blood was drawn from their hearts under anesthesia and the aortas were cut to confirm death.

All animal care procedures and experiments were approved by the Animal Experiment Committee of the University of Tokyo (approval number: Medical-P20-009) and the authors complied with the ARRIVE guidelines. All experiments were performed in accordance with relevant guidelines and regulations.

Mouse hindlimb fixation model

Mouse hindlimbs were wrapped with surgical tape (3 M Japan, Tokyo, Japan) and aluminum wires (DAIDOHANT Co., Ltd., Osaka, Japan) was used to fix both sides, in accordance with the protocol outlined in a previous study⁵³. All mice used in the experiment were wired at the same time and at the same week of age, defined as 0d just before winding. After immobilization, the mice were allowed to move, drink, and eat freely in the cage using their forelimbs.

Castration and testosterone administration

The testes of 8-week-old mice were removed and testosterone (Testosterone Propionate; TOKYO CHEMICAL INDUSTRY CO., LTD., Tokyo, Japan) was administered to some mice as described in our previous study⁵². Testosterone was dissolved in safflower oil (Wako, Osaka, Japan) and injected subcutaneously at 50 mg/kg twice weekly. In the sham group, the abdomen was opened under anesthesia, but closed without further surgical manipulation.

Measurements of muscle strength

1. Grip strength test

The mouse grip strength was measured using a grip strength tester (MK-380CM/R; Muromachi Kikai Co., Ltd., Tokyo, Japan). Briefly, mice were instructed to grasp a 12×8 cm wire mesh connected to the grip strength tester with all four limbs, and their tails were pulled backward while holding the mesh in this position. Each mouse was measured in two sets of five repetitions and the average values, except for the maximum and minimum values, were calculated for each set.

2. Wire Hang test

A wire mesh was placed on top of a 20 cm high translucent acrylic case. After the mouse was placed on top, the wire mesh was inverted, the mouse was suspended upside down, and the time to fall was measured. Three measurements were recorded for each mouse, and the maximum value was used. Measurements were terminated at 180 s.

Measurement of IL-6 concentration

Blood was collected from the thoracic aorta, mixed with heparin in an Eppendorf tube, and centrifuged at 4 °C, 4500 rpm for 10 min to collect plasma. The plasma IL-6 concentrations were measured using a Quantikine ELISA Mouse IL-6 Immunoassay in accordance with the manufacturer's protocol (M6000B, R&D Systems Inc.).

Measurement of the muscle cross-sectional area (CSA)

Skeletal muscle fibers can be broadly classified into slow (type I) and fast (type II) twitch fibers⁵⁴. As sarcopenia is characterized by selective atrophy of fast muscle fibers⁵⁵, the gastrocnemius muscle (a primarily fast muscle) was used for this analysis.

Gastrocnemius muscles were dissected and quickly frozen. Serial 10- μ m thick sections were made around the muscle belly (the area of maximum CSA) and hematoxylin-eosin (HE) stained (Applied Medical Research Laboratory, Osaka, Japan). The CSAs of the muscle fibers were determined by tracing the circumference of at least 100 randomly selected muscle fibers per specimen. The prepared specimens were observed using a fluorescence microscope (APX100, Evident, Tokyo, Japan; BZ-X810, Keyence, Osaka, Japan), and the microscopic images were analyzed using ImageJ 1.52a software (National Institutes of Health, MD, USA, <https://imagej.nih.gov/ij/>)⁵⁶.

Immunohistochemical analysis of muscle tissue

Immunohistochemical analysis was performed on frozen sections. The specimens were prefixed in 4% PFA and mixed with 3% H₂O₂/MetOH (Agilent), avidin/biotin solution (Agilent), and 2% bovine serum albumin (Sigma-Aldrich), followed by overnight incubation with the primary antibody CD68 (dilution 1:100, Bio-Rad). After washing, the glass slides were incubated with Alexa-488 streptavidin (Jackson ImmunoResearch) and Biotin-SP Donkey Anti-Rat IgG (Jackson ImmunoResearch), and the nuclei were incubated with DAPI (1:5000, Sigma-Aldrich) for contrast staining.

When quantifying IHC results for CD68, sections contain at least 50–100 skeletal muscle fibers were selected and only staining located near DAPI (within 5 µm) were measured as previously reported⁵⁷.

RNA extraction from skeletal muscle and quantitative PCR (qPCR)

RNA was extracted from gastrocnemius muscle tissues. Tissues were homogenized using a cell destroyer (#PS1000; Bio Medical Science, Tokyo, Japan) in RNAlater Stabilization Solution (Invitrogen), and total RNA was extracted using an RNeasy Mini Kit (#74106; Qiagen). cDNA was synthesized by reverse transcription using an Omniscript RT Kit (#205110; Qiagen) and oligo (dT) primers (Invitrogen). qPCR was performed using the SYBR Green method with Fast SYBR Green PCR Master Mix (Applied Biosystems) as the reagent and a StepOnePlus Real-Time PCR System (Applied Biosystems). GAPDH was used for standardization. The primer sequences used were as follows: *GAPDH*; 5'-AACTTTGGCATTGTGGAAGG-3' (forward) and 5'-ACACATTGGGGGTA GGAACA-3' (reverse), *C/EBPδ*; 5'-CTCCAGGGTCTAAATACATAGC-3' (forward) and 5'-CTCACAGCAGT CCACAAG-3' (reverse), *Myostatin*; 5'-CTCCAGAATAGAAGCCATA-3' (forward) and 5'-GCAGAAGTTGTC TTATAGC-3' (reverse), *F4/80*; 5'-TTGGCCAAGATTCTCTTCCT-3' (forward) and 5'-TCACTGCCTCCACT AGCATC-3' (reverse), *IL-6*; 5'-CAATGCTCTCCTAACAGATAAG-3' (forward) and 5'-AGGCATAACGCACT AGGT-3' (reverse), *Atrogin1*; 5'-GAGGCAGATTCGCAAGCGTTTGAT-3' (forward) and 5'-TCCAGGAGAG AATGTGGCAGTGTT-3' (reverse), *MuRF1*; 5'-AGTGTCCATGTCTGGAGGTCGTTT-3' (forward) and 5'-A CTGGAGCACTCCTGCTTGTAGAT-3' (reverse).

Western blotting (WB)

Gastrocnemius muscle was homogenized in T-PER (Thermo Fisher Scientific) with a protease inhibitor cocktail (Roche) and a phosphatase inhibitor cocktail (Roche) that effectively lysed membrane and intercellular protein⁵⁸. The protein concentration was determined using a BCA protein assay kit (Thermo Fisher Scientific). Briefly, 10 µg of protein sample per well was transferred to 7.5% polyacrylamide gels (Wako) and then transferred to a PVDF membrane by Sodium dodecyl-sulfate polyacrylamide gel electrophoresis (SDS-PAGE). Membranes were incubated overnight with the following primary antibodies: anti-AR (dilution 1:1000, Santa Cruz) and anti-ubiquitin (1:1000, Cell Signaling Technology)⁵⁹. The membranes were washed and incubated with the corresponding horseradish peroxidase-conjugated secondary antibodies (GE Healthcare). Bands were detected using ECL Prime (GE Healthcare) and quantified using ImageJ software.

We also measured the whole protein simultaneously. Briefly, 10 µg of protein sample per well was transferred to 10% polyacrylamide gels (Wako) and stained with Coomassie Brilliant Blue (TaKaRa). Analysis was performed using ImageJ software.

Statistical analyses

All data are presented as the mean ± standard error of the mean (SEM). Statistical comparisons between the two groups were performed using the Mann–Whitney *U* test. Multiple group comparisons were performed using analysis of variance with a post-hoc Tukey test. All data were analyzed using Prism 6.0 (GraphPad Software, <https://www.graphpad.com/>). *P*-values < 0.05 were considered significant.

Data availability

The datasets generated and/or analyzed during the current study are available from corresponding author on reasonable request.

Received: 4 March 2024; Accepted: 19 March 2025

Published online: 27 March 2025

References

1. Tieland, M., Trouwborst, I. & Clark, B. C. Skeletal muscle performance and ageing. *J. Cachexia Sarcopenia Muscle*. **9**, 3–19. <https://doi.org/10.1002/jcsm.12238> (2018).
2. Cruz-Jentoft, A. J. & Sayer, A. A. Sarcopenia. *Lancet* **393**, 2636–2646. [https://doi.org/10.1016/s0140-6736\(19\)31138-9](https://doi.org/10.1016/s0140-6736(19)31138-9) (2019).
3. Cohen, S., Nathan, J. A. & Goldberg, A. L. Muscle wasting in disease: Molecular mechanisms and promising therapies. *Nat. Rev. Drug Discov.* **14**, 58–74. <https://doi.org/10.1038/nrd4467> (2015).
4. Son, B. K. et al. Association between inflammatory potential of the diet and sarcopenia/its components in community-dwelling older Japanese men. *Arch. Gerontol. Geriatr.* **97**, 104481. <https://doi.org/10.1016/j.archger.2021.104481> (2021).
5. Visser, M. et al. Relationship of interleukin-6 and tumor necrosis factor-α with muscle mass and muscle strength in elderly men and women: The health ABC study. *J. Gerontol. Biol. Sci. Med. Sci.* **57**, M326–M332. <https://doi.org/10.1093/gerona/57.5.m326> (2002).
6. Langen, R. C. J. et al. Tumor necrosis factor-α inhibits myogenic differentiation through myoD protein destabilization. *FASEB J.* **18**, 227–237. <https://doi.org/10.1096/fj.03-0251com> (2004).
7. Zhang, L. et al. Pharmacological inhibition of myostatin suppresses systemic inflammation and muscle atrophy in mice with chronic kidney disease. *FASEB J.* **25**, 1653–1663. <https://doi.org/10.1096/fj.10-176917> (2011).
8. Ferrucci, L. & Fabbri, E. Inflammageing: Chronic inflammation in ageing, cardiovascular disease, and frailty. *Nat. Rev. Cardiol.* **15**, 505–522. <https://doi.org/10.1038/s41569-018-0064-2> (2018).

9. Chung, H. Y. et al. Molecular inflammation: Underpinnings of aging and age-related diseases. *Ageing Res. Rev.* **8**, 18–30. <https://doi.org/10.1016/j.arr.2008.07.002> (2009).
10. Chhetri, J. K. et al. Chronic inflammation and sarcopenia: A regenerative cell therapy perspective. *Exp. Gerontol.* **103**, 115–123. <https://doi.org/10.1016/j.exger.2017.12.023> (2018).
11. Tajar, A. et al. Characteristics of androgen deficiency in late-onset hypogonadism: Results from the European male aging study (EMAS). *J. Clin. Endocrinol. Metab.* **97**, 1508–1516. <https://doi.org/10.1210/jc.2011-2513> (2012).
12. Amory, J. K. Study clarifies associations between hypogonadism and health in aging men. *Asian J. Androl.* **14**, 809–810. <https://doi.org/10.1038/aja.2012.78> (2012).
13. Ferrando, A. A. et al. Testosterone administration to older men improves muscle function: Molecular and physiological mechanisms. *Am. J. Physiol. Endocrinol. Metab.* **282**, E601–607. <https://doi.org/10.1152/ajpendo.00362.2001> (2002).
14. Rossetti, M. L., Steiner, J. L. & Gordon, B. S. Androgen-mediated regulation of skeletal muscle protein balance. *Mol. Cell. Endocrinol.* **447**, 35–44. <https://doi.org/10.1016/j.mce.2017.02.031> (2017).
15. De Naeyer, H. et al. Androgenic and estrogenic regulation of Atrogin-1, MuRF1 and myostatin expression in different muscle types of male mice. *Eur. J. Appl. Physiol.* **114**, 751–761. <https://doi.org/10.1007/s00421-013-2800-y> (2014).
16. Deane, C. S. et al. Impaired hypertrophy in myoblasts is improved with testosterone administration. *J. Steroid Biochem. Mol. Biol.* **138**, 152–161. <https://doi.org/10.1016/j.jsbmb.2013.05.005> (2013).
17. Hughes, D. C. et al. Testosterone enables growth and hypertrophy in fusion impaired myoblasts that display myotube atrophy: Deciphering the role of androgen and IGF-I receptors. *Biogerontology* **17**, 619–639. <https://doi.org/10.1007/s10522-015-9621-9> (2016).
18. White, J. P. et al. Testosterone regulation of Akt/mTORC1/FoxO3a signaling in skeletal muscle. *Mol. Cell. Endocrinol.* **365**, 174–186. <https://doi.org/10.1016/j.mce.2012.10.019> (2013).
19. Kovacheva, E. L., Hikim, A. P., Shen, R., Sinha, I. & Sinha-Hikim, I. Testosterone supplementation reverses sarcopenia in aging through regulation of myostatin, c-Jun NH2-terminal kinase, Notch, and Akt signaling pathways. *Endocrinology* **151**, 628–638. <https://doi.org/10.1210/en.2009-1177> (2010).
20. Malkin, C. J. et al. The effect of testosterone replacement on endogenous inflammatory cytokines and lipid profiles in hypogonadal men. *J. Clin. Endocrinol. Metab.* **89**, 3313–3318. <https://doi.org/10.1210/jc.2003-031069> (2004).
21. Bellido, T. et al. Regulation of interleukin-6, osteoclastogenesis, and bone mass by androgens. The role of the androgen receptor. *J. Clin. Invest.* **95**, 2886–2895. <https://doi.org/10.1172/jci117995> (1995).
22. Johansen, J. A., Breedlove, S. M. & Jordan, C. L. Androgen receptor expression in the levator Ani muscle of male mice. *J. Neuroendocrinol.* **19**, 823–826. <https://doi.org/10.1111/j.1365-2826.2007.01592.x> (2007).
23. Sinha-Hikim, I., Taylor, W. E., Gonzalez-Cadavid, N. F., Zheng, W. & Bhasin, S. Androgen receptor in human skeletal muscle and cultured muscle satellite cells: Up-regulation by androgen treatment. *J. Clin. Endocrinol. Metab.* **89**, 5245–5255. <https://doi.org/10.1210/jc.2004-0084> (2004).
24. Monks, D. A., O'Bryant, E. L. & Jordan, C. L. Androgen receptor immunoreactivity in skeletal muscle: Enrichment at the neuromuscular junction. *J. Comp. Neurol.* **473**, 59–72. <https://doi.org/10.1002/cne.20088> (2004).
25. Chambon, C. et al. Myocytic androgen receptor controls the strength but not the mass of limb muscles. *Proc. Natl. Acad. Sci.* **107**, 14327–14332. <https://doi.org/10.1073/pnas.1009536107> (2010).
26. Ophoff, J. et al. Androgen signaling in myocytes contributes to the maintenance of muscle mass and fiber type regulation but not to muscle strength or fatigue. *Endocrinology* **150**, 3558–3566. <https://doi.org/10.1210/en.2008-1509> (2009).
27. Son, B. K. et al. Low-intensity exercise suppresses CCAAT/enhancer-binding protein Δ /myostatin pathway through androgen receptor in muscle cells. *Gerontology* **65**, 397–406. <https://doi.org/10.1159/000499826> (2019).
28. Zhang, L. et al. Stat3 activation links a C/EBP δ to myostatin pathway to stimulate loss of muscle mass. *Cell. Metab.* **18**, 368–379. <https://doi.org/10.1016/j.cmet.2013.07.012> (2013).
29. Zimmers, T. A. et al. Induction of cachexia in mice by systemically administered myostatin. *Science* **296**, 1486–1488. <https://doi.org/10.1126/science.1069525> (2002).
30. Furrer, R. & Handschin, C. Muscle wasting diseases: Novel targets and treatments. *Annu. Rev. Pharmacol. Toxicol.* **59**, 315–339. <https://doi.org/10.1146/annurev-pharmtox-010818-021041> (2019).
31. Dubois, V. et al. A satellite cell-specific knockout of the androgen receptor reveals myostatin as a direct androgen target in skeletal muscle. *FASEB J.* **28**, 2979–2994. <https://doi.org/10.1096/fj.14-249748> (2014).
32. Kawada, S., Okuno, M. & Ishii, N. Testosterone causes decrease in the content of skeletal muscle myostatin. *Int. J. Sport Health Sci.* **4**, 44–48. <https://doi.org/10.5432/ijshs.4.44> (2006).
33. Hulmi, J. J. et al. Androgen receptors and testosterone in men—effects of protein ingestion, resistance exercise and fiber type. *J. Steroid Biochem. Mol. Biol.* **110**, 130–137. <https://doi.org/10.1016/j.jsbmb.2008.03.030> (2008).
34. Ghaibour, K. et al. Androgen receptor coordinates muscle metabolic and contractile functions. *J. Cachexia Sarcopenia Muscle* **14**, 1707–1720. <https://doi.org/10.1002/jcsm.13251> (2023).
35. Allen, D. L., Cleary, A. S., Hanson, A. M., Lindsay, S. F. & Reed, J. M. CCAAT/enhancer binding protein- δ expression is increased in fast skeletal muscle by food deprivation and regulates myostatin transcription in vitro. *Am. J. Physiol. Regul. Integr. Comp. Physiol.* **299**, R1592–R1601. <https://doi.org/10.1152/ajpregu.00247.2010> (2010).
36. Penner, G., Gang, G., Sun, X., Wray, C. & Hasselgren, P. O. C/EBP DNA-binding activity is upregulated by a glucocorticoid-dependent mechanism in septic muscle. *Am. J. Physiol. Regul. Integr. Comp. Physiol.* **282**, R439–R444. <https://doi.org/10.1152/ajprgu.00512.2001> (2002).
37. Yang, H. et al. Expression and activity of C/EBP β and Δ are upregulated by dexamethasone in skeletal muscle. *J. Cell. Physiol.* **204**, 219–226. <https://doi.org/10.1002/jcp.20278> (2005).
38. Allen, D. L. & Unterman, T. G. Regulation of myostatin expression and myoblast differentiation by FoxO and SMAD transcription factors. *Am. J. Physiol. Cell. Physiol.* **292**, C188–C199. <https://doi.org/10.1152/ajpcell.00542.2005> (2007).
39. Jimenez-Gutierrez, G. E. et al. Molecular mechanisms of inflammation in sarcopenia: Diagnosis and therapeutic update. *Cells* **11**, 2359. <https://doi.org/10.3390/cells11152359> (2022).
40. Zhang, X. et al. Immune system and sarcopenia: Presented relationship and future perspective. *Exp. Gerontol.* **164**, 111823. <https://doi.org/10.1016/j.exger.2022.111823> (2022).
41. Balamurugan, K. & Sterneck, E. The many faces of C/EBP δ and their relevance for inflammation and cancer. *Int. J. Biol. Sci.* **9**, 917–933. <https://doi.org/10.7150/ijbs.7224> (2013).
42. Spek, C. A., Abernethy, H. L., Butler, J. M., De Vos, A. F. & Duitman, J. CEBPD potentiates the macrophage inflammatory response but CEBPD knock-out macrophages fail to identify CEBPD-dependent pro-inflammatory transcriptional programs. *Cells* **10**, 2233. <https://doi.org/10.3390/cells10092233> (2021).
43. Balamurugan, K. et al. C/EBP δ links IL-6 and HIF-1 signaling to promote breast cancer stem cell-associated phenotypes. *Oncogene* **38**, 3765–3780. <https://doi.org/10.1038/s41388-018-0516-5> (2019).
44. Mohamad, N. V. et al. The relationship between Circulating testosterone and inflammatory cytokines in men. *Aging Male*. **22**, 129–140. <https://doi.org/10.1080/13685538.2018.1482487> (2019).
45. Akira, S. et al. A nuclear factor for IL-6 expression (NF-IL6) is a member of a C/EBP family. *EMBO J.* **9**, 1897–1906. <https://doi.org/10.1002/j.1460-2075.1990.tb08316.x> (1990).
46. Kawanishi, N., Funakoshi, T. & Machida, S. Time-course study of macrophage infiltration and inflammation in cast immobilization-induced atrophied muscle of mice. *Muscle Nerve* **57**, 1006–1013. <https://doi.org/10.1002/mus.26061> (2018).

47. Hirata, Y. et al. A Piezo1/KLF15/IL-6 axis mediates immobilization-induced muscle atrophy. *J. Clin. Investig.* **132**, 1–13. <https://doi.org/10.1172/jci154611> (2022).
48. Madaro, L. et al. Denervation-activated STAT3–IL-6 signalling in fibro-adipogenic progenitors promotes myofibres atrophy and fibrosis. *Nat. Cell. Biol.* **20**, 917–927. <https://doi.org/10.1038/s41556-018-0151-y> (2018).
49. Alford, E. K., Roy, R. R., Hodgson, J. A. & Edgerton, V. R. Electromyography of rat Soleus, medial gastrocnemius, and tibialis anterior during Hind limb suspension. *Exp. Neurol.* **96**, 635–649. [https://doi.org/10.1016/0014-4886\(87\)90225-1](https://doi.org/10.1016/0014-4886(87)90225-1) (1987).
50. Cannavino, J., Brocca, L., Sandri, M., Bottinelli, R. & Pellegrino, M. A. PGC1- α over-expression prevents metabolic alterations and soleus muscle atrophy in hindlimb unloaded mice. *J. Physiol.* **592**, 4575–4589. <https://doi.org/10.1113/jphysiol.2014.275545> (2014).
51. Okamoto, T., Torii, S. & Machida, S. Differential gene expression of muscle-specific ubiquitin ligase MAFbx/Atrogin-1 and MuRF1 in response to immobilization-induced atrophy of slow-twitch and fast-twitch muscles. *J. Physiol. Sci.* **61**, 537–546. <https://doi.org/10.1007/s12576-011-0175-6> (2011).
52. Son, B. K., Kojima, T., Ogawa, S. & Akishita, M. Testosterone inhibits aneurysm formation and vascular inflammation in male mice. *J. Endocrinol.* **241**, 307–317. <https://doi.org/10.1530/joe-18-0646> (2019).
53. Saitou, K. et al. Local cyclical compression modulates macrophage function in situ and alleviates immobilization-induced muscle atrophy. *Clin. Sci. (Lond.)* **132**, 2147–2161. <https://doi.org/10.1042/cs20180432> (2018).
54. Talbot, J. & Maves, L. Skeletal muscle fiber type: Using insights from muscle developmental biology to dissect targets for susceptibility and resistance to muscle disease. *WIREs Dev. Biol.* **5**, 518–534. <https://doi.org/10.1002/wdev.230> (2016).
55. Lexell, J., Taylor, C. C. & Sjöström, M. What is the cause of the ageing atrophy? Total number, size and proportion of different fiber types studied in whole Vastus lateralis muscle from 15- to 83-year-old men. *J. Neurol. Sci.* **84**, 275–294. [https://doi.org/10.1016/0022-510x\(88\)90132-3](https://doi.org/10.1016/0022-510x(88)90132-3) (1988).
56. Schneider, C. A., Rasband, W. S. & Eliceiri, K. W. NIH image to imageJ: 25 years of image analysis. *Nat. Methods.* **9**, 671–675. <https://doi.org/10.1038/nmeth.2089> (2012).
57. Kosmac, K. et al. Immunohistochemical identification of human skeletal muscle macrophages. *Bio Protoc.* <https://doi.org/10.2176/9/BioProtoc.2883> (2018).
58. Holdman, X. B. et al. Upregulation of EGFR signaling is correlated with tumor stroma remodeling and tumor recurrence in FGFR1-driven breast cancer. *Breast Cancer Res.* **17** <https://doi.org/10.1186/s13058-015-0649-1> (2015).
59. Paul, P. K. et al. The E3 ubiquitin ligase TRAF6 intercedes in starvation-induced skeletal muscle atrophy through multiple mechanisms. *Mol. Cell. Biol.* **32**, 1248–1259. <https://doi.org/10.1128/mcb.06351-11> (2012).

Acknowledgements

We thank Ms. Hiroko Sasakawa for helpful comments and suggestions. Dr. Yasuhiro Sawada and Dr. Naoyoshi Sakitani of the National Rehabilitation Center for Persons with Disabilities provided invaluable assistance in the experimental development of the immobilization-induced muscle atrophy mouse model. We express our deepest gratitude to the reviewers.

Author contributions

All authors made substantial contributions to the conception and design, establishment of animal models, and analysis and interpretation of the data in this study. M.O., B.K.S., and M.A. conceived the study; M.O., Z.S., K.T., and M.N.H. collected the data; and M.O. analyzed the data and wrote the manuscript. M. O., B.K.S., S.O. and M.A. read and approved the final manuscript.

Funding

This study was supported by Grants-in-Aid for Scientific Research from the Ministry of Education, Culture, Sports, Science, and Technology of Japan (19K07931, 23H02811) and 8th the Japan Geriatrics Society (JGS) Research Grant Award in Geriatrics and Gerontology (2023).

Declarations

Competing interests

The authors declare no competing interests.

Ethical standards

All of the animal care procedures and experiments were approved by the Animal Experiment Committee of the University of Tokyo.

Additional information

Supplementary Information The online version contains supplementary material available at <https://doi.org/10.1038/s41598-025-95115-6>.

Correspondence and requests for materials should be addressed to B.-K.S.

Reprints and permissions information is available at www.nature.com/reprints.

Publisher's note Springer Nature remains neutral with regard to jurisdictional claims in published maps and institutional affiliations.

Open Access This article is licensed under a Creative Commons Attribution-NonCommercial-NoDerivatives 4.0 International License, which permits any non-commercial use, sharing, distribution and reproduction in any medium or format, as long as you give appropriate credit to the original author(s) and the source, provide a link to the Creative Commons licence, and indicate if you modified the licensed material. You do not have permission under this licence to share adapted material derived from this article or parts of it. The images or other third party material in this article are included in the article's Creative Commons licence, unless indicated otherwise in a credit line to the material. If material is not included in the article's Creative Commons licence and your intended use is not permitted by statutory regulation or exceeds the permitted use, you will need to obtain permission directly from the copyright holder. To view a copy of this licence, visit <http://creativecommons.org/licenses/by-nc-nd/4.0/>.

© The Author(s) 2025